Performance Analysis and Code Optimization of Low Density Parity-Check Codes on Rayleigh Fading Channels*

Jilei Hou, Paul H. Siegel and Laurence B. Milstein
Department of Electrical and Computer Engineering
University of California, San Diego
La Jolla, CA 92093-0407
{jhou,psiegel,milstein}@cwc.ucsd.edu

Abstract

A numerical method has recently been presented to determine the noise thresholds of low density parity-check (LDPC) codes that employ the message passing decoding algorithm on the additive white Gaussian noise (AWGN) channel. In this paper, we extend this technique to the uncorrelated flat Rayleigh fading channel. Using a nonlinear code optimization technique, we optimized irregular LDPC codes for the uncorrelated Rayleigh fading channel. The thresholds of the optimized irregular LDPC codes are very close to the Shannon limit for this channel. For example, at rate 1/3, the optimized irregular LDPC code has a threshold only 0.08dB away from the channel capacity.

1 Introduction

Recent advances [1][2] in error correcting codes have shown that, using the message passing decoding algorithm, irregular low density parity-check (LDPC) codes can achieve reliable transmission at signal-to-noise ratios (SNR) extremely close to the Shannon limit on the additive white Gaussian noise (AWGN) channel, outperforming turbo codes of the same block size and code rate. LDPC codes have certain advantages, such as simple descriptions of their code structure and fully parallelizable decoding implementations. Moreover, they are amenable to theoretical decoding analysis. With iterative message passing decoders, LDPC codes exhibit an interesting threshold effect [1][3]: if the noise level of the channel is smaller than a certain threshold, the bit error probability goes to zero as the block size goes to infinity; if the noise level is above the threshold, the probability of error is always bounded away from zero. Richardson, $et\,al.$ [1] developed a numerical technique, called $density\ evolution$, to analyze the performance of the message passing decoding algorithm on the AWGN channel, enabling the determination of thresholds to any desired degree of accuracy. In this paper, we extend this technique to the uncorrelated flat Rayleigh fading channel.

The code optimization of irregular LDPC codes is a nonlinear cost function minimization problem, a problem where differential evolution has been shown to be very effective and robust [4]. This technique has been successfully applied to the design of good irregular LDPC codes for both the erasure channel [4] and the AWGN channel [2]. We show that this technique is also very effective in the code optimization of irregular LDPC codes for the uncorrelated Rayleigh fading channel, and the threshold values of the optimized codes are extremely close to the capacity of this channel.

*This work was sponsored by the National Science Foundation under Grant NCR-9725568.

2 Low Density Parity-Check (LDPC) codes

An LDPC code is a linear block code specified by a very sparse parity-check matrix. As a linear block code, an LDPC code can be represented by a bipartite graph. Suppose the low density parity-check matrix H has N columns and M rows; the corresponding bipartite graph consists of N bit nodes, M check nodes, and a certain number of edges. Each bit node, called "left node," represents a bit of the codeword. Each check node, called "right node," represents a parity check of the code. An edge exists between a bit node and a check node if and only if there is a 1 in the corresponding entry in the parity-check matrix. We refer to the corresponding bit node and check node as the left and right neighbor nodes of the edge.

Regular LDPC codes are those for which all nodes of the same type have the same degree, where the degree of a node is the number of edges for which it is a neighbor node. A (j,k) regular LDPC code has a bipartite graph in which all bit nodes have degree j and all check nodes have degree k. Correspondingly, in the parity-check matrix H, all the column weights are j and all the row weights are k.

For irregular LDPC codes, the bit nodes (correspondingly the check nodes) can have different degrees. We say an edge has left (resp., right) degree i if its left (resp., right) neighbor node has degree i. An irregular LDPC code ensemble is specified by a degree sequence (λ, ρ) or its corresponding generating functions $\lambda(x) = \sum_{i=2}^{d_{lmax}} \lambda_i x^{i-1}$ and $\rho(x) = \sum_{i=2}^{d_{rmax}} \rho_i x^{i-1}$, where λ_i (resp., ρ_i) is the fraction of edges with left (resp., right) degree i and d_{lmax} (resp., d_{rmax}) is the maximal left (resp., right) degree of any edge.

3 Decoding Analysis

Firstly, we briefly review the decoding algorithm [2][5] for LDPC codes. For each edge of the underlying bipartite graph, the decoding algorithm iteratively updates two types of log a posteriori probability ratio (LAPPR) messages, q and r. The quantity q is the message sent from the bit node to the check node along a connecting edge e, which is expressed as $q = \log \frac{p(x=0|t)}{p(x=1|t)}$, where t denotes all the messages coming from the channel and the edges connected to the bit node, other than edge e. The quantity r is the message sent from the check node to the bit node along an edge e, which is defined as $r = \log \frac{p(x=0|v)}{p(x=1|v)}$, where v denotes the messages coming from the edges connected to the check node, other than edge e.

After l such iterations, the algorithm would produce the exact LAPPRs of all the bits if the bipartite graph defined by the parity-check matrix contains no loops of length up to $2l$ [5]. If we assume that the graph is loop-free, we can analyze the decoding algorithm directly because the incoming messages to every node are independent. Also, by the general concentration theorem of [1], for almost all the graphs in a code ensemble (λ, ρ) and almost all inputs, the decoder performance will converge to that of a corresponding loop-free graph as the codeword length approaches infinity.

Based on the assumption above, the following decoding analysis tries to track the $average$ fraction of incorrect messages that is passed in each iteration of the decoding algorithm. Here, the fraction of incorrect messages is averaged over all the bits of a codeword.

First, we consider a regular (j, k) LDPC code. Since LDPC codes are linear block codes, we can assume that the all-zero codeword is sent and BPSK modulation $(0 \rightarrow 1,\ 1 \rightarrow -1)$ is used. Considering the message passed from the bit node to the check node, we have [2]

$$q = q_0 + \sum_{i=1}^{j-1} r_i \,, \tag{1}$$

where q_0 is the initial message conditioned on the channel output, and r_i , $i = 1, ..., j-1$, are the incoming LAPPR messages from all the incident edges, other than edge e. Since q_0 and r_i are independent random variables, the density function of q is the convolution of the density functions of all the elements in (1). This convolution can be efficiently computed in the Fourier domain. Let P_0 denote the density of q_0, P_l denote the density of q after l iterations, and R_l denote the density of r after l iterations. Letting F denote the Fourier transform operation,

$$P_l = F^{-1}\left(F\left(P_0\right)\left(F\left(R_{l-1}\right)\right)^{j-1}\right), \tag{2}$$

where $R_0(r)$ can be set to Δ_0, and Δ_0 is defined as 1 if $r = 0$ and 0 if $r \neq 0$. We can write $P_l = P_l^1 + P_l^0$, where P_l^1 is supported on $(-\infty, 0]$ and P_l^0 is supported on $[0, \infty)$. Therefore, the fraction of incorrect messages after l iterations can be defined as

$$Pe(l) = \int_{-\infty}^{0} P_l(z)dz\,. \tag{3}$$

On the other hand, considering the message r passed from the check node to the bit node r, we have [2]

$$\tanh\frac{r}{2} = \prod_{i=1}^{k-1}\tanh\frac{q_i}{2}\,, \tag{4}$$

where q_i , $i = 1, ..., k-1$ are the incoming LAPPRs from the neighbor edges, other than edge e. To use the same method as described for the bit node to calculate the density function R_l, we need to apply logarithm operations on both sides of (4) to change the product into a summation,

$$(sgn_r\,,\,\log\left|\tanh\frac{r}{2}\right|) = \sum_{i=1}^{k-1}(sgn_{q_i}\,,\,\log\left|\tanh\frac{q_i}{2}\right|)\,, \tag{5}$$

where the sign function $sgn_x = 0$ if $x \geq 0$, and $sgn_x = 1$ otherwise. Note that the summation for (5) is the mod-2 summation of the sign parts and the real summation of the magnitude parts. Therefore, the density of r can be computed in the Fourier domain in a manner similar to the computation of the density of q in (2).

This two-phase computation algorithm, called density evolution, makes it possible to track the fraction of incorrect messages, $Pe(l)$. At a certain noise level, we can run this algorithm iteratively until the error probability $Pe(l)$ either goes to zero or stops at a finite probability of error. The threshold, σ^*, denotes the supremum of all values of the noise level σ such that $\lim_{l\to\infty} Pe(l) = 0$, where σ is the standard deviation of the noise.

The density evolution algorithm can be extended to the irregular LDPC codes with only minor modifications, taking into consideration the irregular degree sequences; for example, at a bit node,

$$P_l = F^{-1}\left(F\left(P_0\right)\cdot\lambda\left(F\left(R_{l-1}\right)\right)\right), \tag{6}$$

where $\lambda(x) = \sum_{i=2}^{d_{lmax}}\lambda_i x^{i-1}$ is as defined above.

For the uncorrelated Rayleigh fading channel, if the code symbol x is mapped into the signal point $w = (1-2x)$, the conditional pdf of the matched filter output y is

$$p(y|w,a) = \frac{1}{\sqrt{2\pi\sigma^2}}\exp\left(-\frac{\left(y - w\cdot a\right)^2}{2\sigma^2}\right), \tag{7}$$

where σ^2 is the variance of the noise, and a is the normalized Rayleigh fading factor with $E[a^2] = 1$ and density function $p(a) = 2a\exp(-a^2)$.

3.1 Ideal side information (SI)

When we have ideal SI, the initial message passed from the bit node to the check node is

$$q_0 = \log \frac{P(x=0|y,a)}{P(x=1|y,a)} = \frac{2}{\sigma^2} y \cdot a \,. \tag{8}$$

In the decoding analysis, assuming $w = 1$, q_0 has the conditional density function

$$P_0\left(q_0|a\right) = \frac{\sigma}{2a\sqrt{2\pi}} \exp\left(-\frac{\left(q_0 - \frac{2a^2}{\sigma^2}\right)^2}{8a^2/\sigma^2} \right) . \tag{9}$$

To get the unconditional density function of q_0, we average (9) over the density function of a,

$$\begin{aligned} P_0(q_0) &= \int_0^\infty \frac{\sigma}{\sqrt{2\pi}} \exp\left(-\frac{\left(q_0 - \frac{2a^2}{\sigma^2}\right)^2}{8a^2/\sigma^2} \right) \exp(-a^2) da \\ &= \frac{\sigma}{\sqrt{2\pi}} \exp\left(\frac{-q_0(\sqrt{2\sigma^2+1}-1)}{2}\right) \int_0^\infty \exp\left(-\frac{\left(\frac{\sigma^2}{2a} q_0 - a\sqrt{2\sigma^2+1}\right)^2}{2\sigma^2} \right) da \,. \end{aligned} \tag{10}$$

3.2 No side information (no SI)

When no SI is available, following [6], we assume that $P(y|w)$ is Gaussian distributed in the region of the most probable y, and we approximate q_0 as

$$q_0 \approx \frac{2}{\sigma^2} y \cdot E[a] \,, \tag{11}$$

where $E[a] = 0.8862$. The corresponding conditional density function is

$$P_0\left(q_0|a\right) = \frac{\sigma}{2E[a]\sqrt{2\pi}} \exp\left(-\frac{\left(q_0 - \frac{2aE[a]}{\sigma^2}\right)^2}{8(E[a])^2/\sigma^2} \right) . \tag{12}$$

Averaging over the density function of a, we get

$$\begin{aligned} P_0(q_0) &= \frac{\sigma\Delta^2}{2E[a]} \exp\left(-\frac{\Delta^2\sigma^2 q_0^2}{4(E[a])^2}\right) \times \\ &\quad \left[\sqrt{\frac{2}{\pi}} \exp\left(-\frac{\Delta^2 q_0^2}{8(E[a])^2}\right) + \frac{\Delta q_0}{E[a]} Q\left(\frac{-\Delta q_0}{2E[a]}\right)\right] , \end{aligned} \tag{13}$$

where $\Delta = \sqrt{\frac{\sigma^2}{2\sigma^2+1}}$ and $Q(x) = \frac{1}{2} erfc(\frac{x}{\sqrt{2}})$.

4 Consistency and Stability

Consistency is an important property associated with the message distribution in the density evolution. As defined in [2], a density function f on $[-\infty, \infty]$ is consistent if it satisfies $f(x) = f(-x)e^x$ for all $x \in [0, \infty]$, and it is shown that the initial message distributions for all the binary-input symmetric channels (including the AWGN channel) discussed in [2] satisfy this condition.

It was shown in [2] that the consistency property is invariant under density evolution, i.e., if P_0 is consistent, then the density functions of P_l and R_l calculated in density evolution are also consistent. It was next proved in [2] that if the density function of P_l is consistent, the average fraction of incorrect messages as defined in (3) is a non-increasing function of l and will always converge to a certain value, which might be zero.

In [2], the consistency property is then used to prove another important property of density evolution, which is summarized as follows: There exists an $\varepsilon > 0$ such that if density evolution is initialized with a consistent message density P_0 satisfying $\int_{-\infty}^{0} P_0(x)dx < \varepsilon$, the fraction of incorrect messages could converge to zero under density evolution if

$$\lambda'(0)\rho'(1) < e^s \tag{14}$$

where the parameter s is defined as

$$s = -\log(2\int_0^\infty P_0(x)e^{-x/2}dx)\,. \tag{15}$$

Conversely, if $\lambda'(0)\rho'(1) > e^s$, then the fraction of incorrect messages is strictly bounded away from 0.

In [2], (14) is referred to as the stability condition for the channel with initial message density P_0. For example, for the AWGN channel, the stability condition is given by [2]

$$\lambda'(0)\rho'(1) < e^{\frac{1}{2\sigma^2}}\,. \tag{16}$$

We now show that the initial message density function of the uncorrelated Rayleigh fading channel with SI also satisfies the consistency property, and then we derive the stability condition for this channel. For the density function of the uncorrelated Rayleigh fading channel with SI, as defined in (10), it is easily verified that

$$\begin{aligned} P_0(q_0) &= \int_0^\infty \tfrac{\sigma}{\sqrt{2\pi}} \exp\left(-\tfrac{\left(q_0-\frac{2a^2}{\sigma^2}\right)^2}{8a^2/\sigma^2}\right)\exp(-a^2)da \\ &= \exp(q_0)\int_0^\infty \tfrac{\sigma}{\sqrt{2\pi}} \exp\left(-\tfrac{\left(-q_0-\frac{2a^2}{\sigma^2}\right)^2}{8a^2/\sigma^2}\right)\exp(-a^2)da \\ &= P_0(-q_0)\exp(q_0)\,, \end{aligned} \tag{17}$$

i.e., the initial message density function of the uncorrelated Rayleigh fading channel with SI satisfies the consistency condition. From (15) and (10), we have

$$\begin{aligned} e^{-s} &= 2\int_0^\infty P_0(q_0)e^{-q_0/2}dq_0 \\ &= 2\int_0^\infty da\tfrac{\sigma}{\sqrt{2\pi}}e^{-a^2}\int_0^\infty \exp(-\tfrac{\left(q_0-\frac{2a^2}{\sigma^2}\right)^2}{8a^2/\sigma^2})e^{-q_0/2}dq_0 \\ &= \int_0^\infty 2a\exp(-(1+\tfrac{1}{2\sigma^2})a^2)da \\ &= 1/(1+\tfrac{1}{2\sigma^2}) \end{aligned}\,, \tag{18}$$

i.e., the stability condition for the uncorrelated Rayleigh fading channel with SI is

$$\lambda'(0)\rho'(1) < 1 + \frac{1}{2\sigma^2}\,. \tag{19}$$

In the next section, we will numerically optimize the degree sequences for this channel, and we will verify empirically that they fulfill condition (19). As to the Rayleigh fading channel without SI, the initial density function (13) does not have the consistency property. We conjecture that this is because the expression (11) for the message, q_0, is only an approximation. Nevertheless, as shown in the numerical results, the density evolution technique for determining the thresholds still works quite well for this channel.

5 Results

5.1 Threshold calculation and code optimization

Using the density evolution technique discussed in Section 3, we can calculate the threshold values of LDPC codes for both the AWGN channel and the uncorrelated Rayleigh fading channel with or without SI. For convenience, in the following results, we will express the threshold by both σ and its corresponding (E_b/N_0)(dB). Since $\sigma^2 = \frac{1}{2R\cdot(E_b/N_0)}$, the threshold can also be defined as the smallest E_b/N_0 such that $\lim_{l\to\infty} Pe(l) = 0$. Fig. 1 compares the thresholds and the simulation results of rate-1/2 regular (3,6) LDPC codes on both the AWGN channel and the uncorrelated Rayleigh fading channel, where both ideal SI and no SI are considered. As shown, the thresholds for regular (3,6) LDPC codes on the AWGN channel, the fading channel with SI, and the fading channel with no SI, are 1.10dB, 3.06dB, and 4.06dB, respectively. The (3,6) LDPC codes used in the simulations are of length 10^5 and 10^6. The numerical threshold results are very consistent with the simulation results, and we conjecture that as the block size goes to infinity, the simulation results will converge to the thresholds. The results show that the regular (3,6) LDPC code suffers a loss of nearly 2dB and 3dB, respectively, in the fading channels with SI and without SI, relative to the AWGN channel.

Combining the density evolution and differential evolution techniques, we searched for good degree sequences with constraints on the maximal left degree d_{lmax} for the uncorrelated Rayleigh fading channel with SI. The differential evolution algorithm that we used in the code optimization is based on [4] with minor modifications. The resulting degree sequences of rate-1/3 codes for the Rayleigh fading channel with SI are shown in Table 1 for $d_{lmax} = 10,\ 16,\ 30,$ and 50. Each column corresponds to one particular degree sequence. For each degree sequence, the coefficients of λ and ρ are given, as well as the threshold σ^*, and the corresponding $(E_b/N_0)^*$ in dB. Also listed is λ_2^*, the maximal value of λ_2 satisfying the stability condition (19). As can be seen, $\lambda_2 < \lambda_2^*$ for every degree sequence in the table, which confirms that these degree sequences satisfy the stability condition. We observe the higher the maximal left degree, the better the performance of the code.

Similar to the results that Richardson, $et\ al.$ [2] obtained for the AWGN channel, the thresholds of the degree sequences optimized for the fading channel with SI are very close to the capacity of this channel (the capacity can be calculated following the method introduced in [7]). At rate 1/3, the capacity of the fading channel with SI is 0.4885dB. The degree sequence with $d_{lmax} = 50$ has the threshold of 0.5712dB, which is only 0.08dB away from the capacity!

For comparison, Table 2 gives the rate-1/3 code sequences that we optimized for the AWGN channel with $d_{lmax} = 10,\ 16,\ 30,$ and 50. The threshold of the code sequence optimized for the AWGN channel with $d_{lmax} = 50$ is only 0.07dB away from the channel capacity.

It is interesting to see how the code sequences optimized for the fading channel with SI perform on the AWGN channel, and vice-versa. We compare the rate-1/3 code sequences optimized for the AWGN channel and the code sequences optimized for the fading channel with SI in Figs. 2. In Fig. 2(a), for each degree sequence, we show the gap between its threshold value for the AWGN channel and the AWGN channel capacity for rate 1/3. In Fig. 2(b), for each degree sequence, we show the gap between its threshold value for the fading channel

with SI and the capacity for that channel for rate 1/3. It can be seen from Fig. 2(a) that the code sequences optimized for the fading channel with SI are also very good sequences on the AWGN channel, e.g., considering the degree sequence with $d_{lmax} = 50$ optimized for the fading channel with SI, its threshold value for the AWGN channel is only 0.16dB away from the channel capacity. Similar results can be observed from Fig. 2(b) for the reverse situation.

5.2 BER Simulation results

As shown in Fig. 1, the threshold values precisely predict the asymptotic performance as the block length of the LDPC codes approaches infinity. We are also interested in the performance of the optimized irregular LDPC codes when finite block size is considered. In the following results, we considered four rate-1/3 LDPC codes at a block size of 3072. The first one, LDPC ir1, is constructed according to the degree sequence with $d_{lmax} = 16$ optimized for the AWGN channel, as shown in Table 2. The degree sequence has thresholds of -0.32dB and 0.78dB on the AWGN channel and the fading channel with SI, respectively. Note that the capacities for these two channels are -0.4954dB and 0.4885dB, respectively. The second one, LDPC ir2, is constructed according to the degree sequence with $d_{lmax} = 16$ optimized for the fading channel with SI, as shown in Table 3, with thresholds of -0.25dB and 0.68dB on the AWGN and fading channel with SI, respectively. The third one, LDPC ir3, is constructed according to a degree sequence[1] with $d_{lmax} = 16$, which has thresholds of -0.18dB and 0.96dB on the AWGN and fading channel with SI, respectively. The last one, a quasi-regular[2] LDPC code R with all bit nodes degree-3, half of the check nodes degree-4, and half of the check nodes degree-5, has thresholds of 0.85dB and 2.13dB on the AWGN channel and the fading channel with SI, respectively. Among the four codes, ir1 has the best threshold on the AWGN channel and ir2 has the best threshold on the fading channel with SI.

Fig. 3(a) compares the simulation results of these four LDPC codes on both an AWGN channel and an uncorrelated Rayleigh fading channel with SI. It is shown that all three irregular LDPC codes achieve excellent performance on both channels. Note that the simulation results reflect the same relative performance as predicted by the computed threshold values. Furthermore, the irregular codes perform much better than the regular code. For example, at a BER of 2×10^{-4}, ir2 outperforms the regular LDPC code on the AWGN channel and fading channel with SI by about 0.7dB and 1.0dB, respectively.

In Fig. 3(b), ir1 and ir2 are compared to a (1,33/31,33/31) turbo code [8] of the same block size and the same code rate on both an AWGN channel and an uncorrelated fading channel with SI. We can see that ir1 and ir2 achieve virtually the same performance as the turbo code. On the AWGN channel, ir1 is slightly better than the other two codes, while on the fading channel with SI, ir2 is slightly better.

6 Conclusions

In this paper, we have shown that the numerical analysis technique for calculating the threshold of the LDPC codes for the AWGN channel can be extended to the uncorrelated flat Rayleigh fading channel. In addition, using the nonlinear optimization technique of differential evolution, we optimized the degree sequences for the uncorrelated Rayleigh fading channel and showed that the threshold values of these degree sequences are extremely close to the capacity

[1]This degree sequence was taken from Sae-Young Chung's web site: http://truth.mit.edu/˜sychung/gaopt.html, which is an irregular LDPC codes design applet for design of good LDPC codes on AWGN channel.

[2]For rate-1/3 (j, k) regular LDPC codes, if we choose $j = 3$, we can not make k to be an integer. Therefore, we choose half of the check nodes degree-4 and half of the check nodes degree-5. We denote this code as a rate-1/3 *quasi-regular* LDPC code.

of this channel. Simulation results for moderate block size showed that the optimized LDPC codes can achieve excellent performance on both the AWGN channel and the Rayleigh fading channel.

The authors wish to thank T. J. Richardson, R. Urbanke, S. Y. Chung, and H. D. Pfister for their helpful comments about the decoding analysis, and K. Tang for providing the simulation results for the turbo codes.

References

[1] T. J. Richardson and R. Urbanke, "The capacity of low-density parity-check codes under message-passing decoding," submitted to *IEEE Trans. Inform. Theory*.

[2] T. J. Richardson, A. Shokrollahi and R. Urbanke, "Design of provably good low-density parity-check codes," submitted to *IEEE Trans. Inform. Theory*.

[3] R. G. Gallager, *Low-Density Parity-Check Codes*. Cambridge, MA: MIT Press, 1963.

[4] A. Shokrollahi and R. Storn, "Design of efficient erasure codes with differential evolution," preprint, 1999.

[5] D. J. C. MacKay, "Good error-correcting codes based on very sparse matrices," *IEEE Trans. Inform. Theory*, vol. 45, no. 2, pp. 399-431, March 1999.

[6] J. Hagenauer, "Viterbi decoding of convolutional codes for fading- and burst- channels," in *Proceedings of Int. Zurich Seminar on Digital Commun.'80*, pp. 1-7, Zurich, Switzerland, March 1980.

[7] E. K. Hall, S. G. Wilson, "Design and analysis of turbo codes on Rayleigh fading channels," *IEEE J-SAC*, vol. 16, no. 2, pp. 160-174, February 1998.

[8] K. Tang, P. H. Siegel and L. B. Milstein, "On the performance of turbo coding for the land mobile channel with delay constraints," in *Proceedings of 33rd Asilomar Conf. SSC'99*, pp. 1659-1665, Pacific Grove, CA, October 1999.

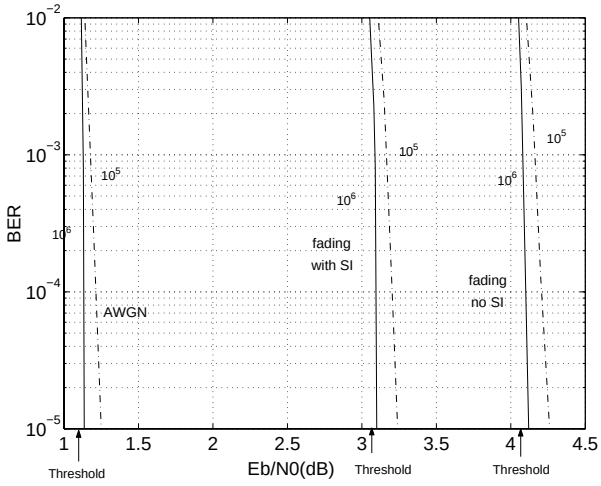

Figure 1: Comparison of thresholds and simulation results for rate-1/2, (3,6) regular LDPC codes on the AWGN channel, and the uncorrelated Rayleigh fading channels with or without SI. The codes used in simulations are of block size 10^5 and 10^6 .

d_{lmax}	10	16	30	50
λ_2^*	0.351321	0.312740	0.279123	0.248068
λ_2	0.328411	0.298433	0.267474	0.237738
λ_3	0.300171	0.245016	0.228605	0.200028
λ_4	0.001721			0.026700
λ_5		0.007173		
λ_6	0.001274	0.167659		
λ_7			0.140199	0.094505
λ_8			0.054426	0.050632
λ_9	0.000662		0.063206	0.028717
λ_{10}	0.367760		0.006163	0.060597
λ_{15}				0.057204
λ_{16}		0.281719		
λ_{29}			0.029347	
λ_{30}			0.210580	0.053621
λ_{49}				0.174248
λ_{50}				0.016010
ρ_4	0.024056	0.004024		
ρ_5	0.974961	0.547412	0.049352	
ρ_6	0.000983	0.448564	0.949897	0.538274
ρ_7			0.000751	0.359720
ρ_8				0.102006
$\sigma*$	1.1220	1.1323	1.1440	1.1468
$\left(\frac{E_b}{N_0}\right)^* dB$	0.7611	0.6817	0.5924	0.5712

Table 1: Good degree sequences of rate-1/3 for the uncorrelated Rayleigh fading channel with SI. For each sequence the threshold value $\sigma*$and the corresponding $\left(\frac{E_b}{N_0}\right)^*$(dB) are given. The maximal value of λ_2 satisfying condition (19), λ_2^*, is given for $\sigma = \sigma^*$and the given $\rho'(1)$. Note that the capacity for this channel at code rate 1/3 is 0.4885 dB.

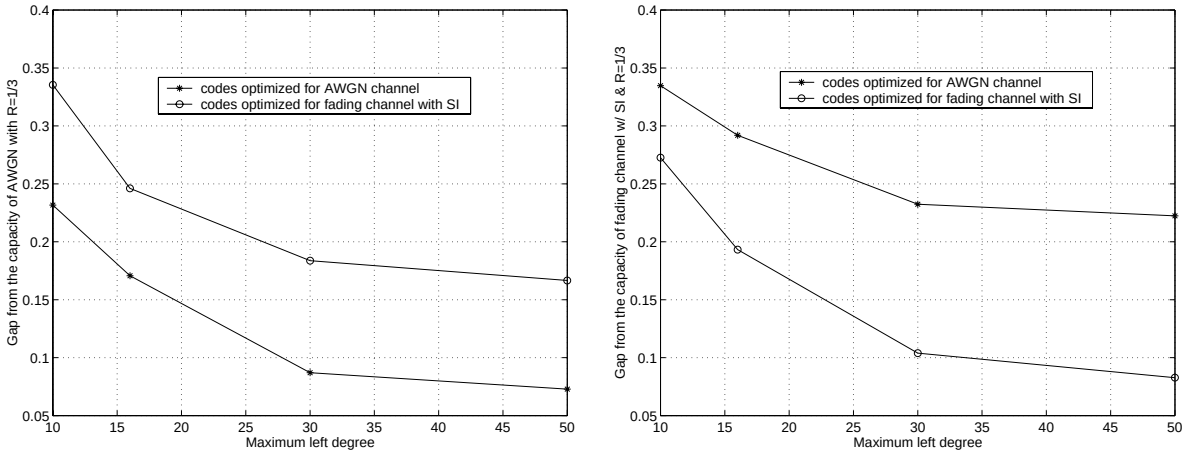

(a) . (b) .

Figure 2: Comparison of the rate-1/3 code sequences optimized for the AWGN channel and the fading channel with SI. Note that the capacity for the AWGN channel at rate 1/3 is -0.4954dB and the capacity for the fading channel with SI at rate 1/3 is 0.4885dB.

d_{lmax}	10	16	30	50
λ_2^*	0.342056	0.298223	0.264470	0.237297
λ_2	0.329076	0.287567	0.256988	0.225792
λ_3	0.261590	0.230039	0.217847	0.207865
λ_4	0.048686	0.002147		0.012662
λ_5		0.068969		
λ_6		0.095590		
λ_7			0.163553	0.107496
λ_8		0.019108	0.061250	0.064003
λ_9			0.044084	0.032510
λ_{10}	0.360648		0.001780	0.012288
λ_{15}				0.100307
λ_{16}		0.296580		
λ_{29}			0.002474	
λ_{30}			0.252024	0.030314
λ_{50}				0.206763
ρ_4	0.000294	0.003426		
ρ_5	0.998683	0.424437		
ρ_6	0.001023	0.572137	0.882069	0.349540
ρ_7			0.114372	0.598609
ρ_8			0.003559	0.051851
$\sigma*$	1.2625	1.2714	1.2837	1.2858
$\left(\frac{E_b}{N_0}\right)^* dB$	-0.2637	-0.3247	-0.4084	-0.4225

Table 2: Good degree sequences of rate-1/3 for the AWGN channels. For each sequence the threshold value $\sigma*$ and the corresponding $\left(\frac{E_b}{N_0}\right)^*$(dB) are given. The maximal value of λ_2 satisfying condition (16), λ_2^*, is given for $\sigma = \sigma^*$and the given $\rho'(1)$. Note that the capacity for this channel at code rate 1/3 is -0.4954 dB.

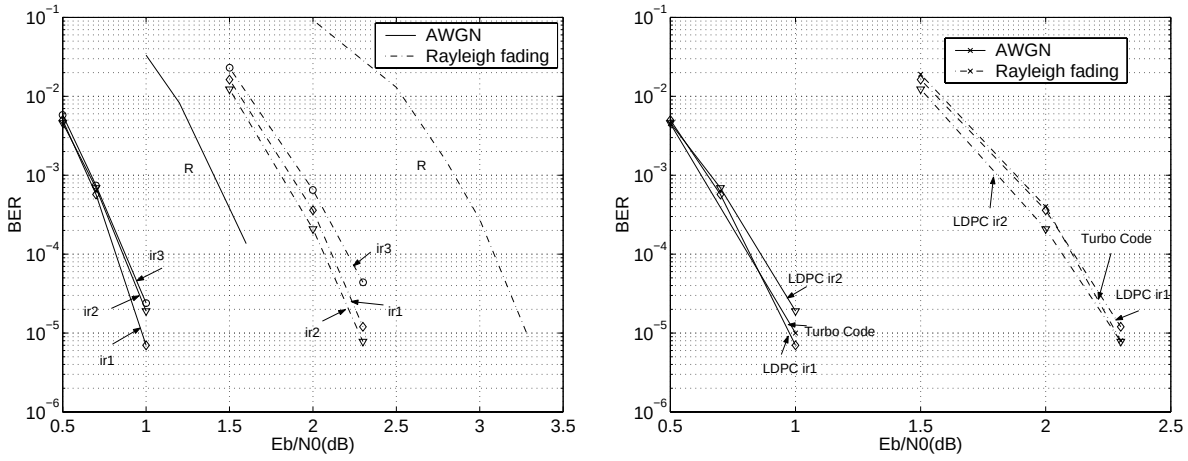

(a) . (b) .

Figure 3: Simulation comparisons of rate-1/3, block size 3072, quasi-regular LDPC code R, irregular LDPC codes ir1, ir2, and ir3, and turbo code on both an AWGN channel and an uncorrelated Rayleigh fading channel with SI.